Local structure of Europium complex oxides

Anastasia Molokova, National Research Nuclear University MEPhI

Supervisor: Dr. Vadim Murzin

September 5, 2019

Abstract

In the present work local structure and valence state of Europium complex oxides were investigated using X-ray absorption spectroscopy (XAS). Gradual change of crystal and local structure during valence transition was considered. Temperature-dependent XAS measurements performed in the range of 10-300K gave us information about local static and dynamic disorder in interatomic distances and Debye-Waller factors.

Content

1. Introduction

Complex oxides of divalent and trivalent europium exhibit interesting properties such as multiferroelectric ordering and crystal and valence transitions [1-3]. First of all I would like to talk about multiferroic materials. Ferroelectric ordering is combined with ferro- or antiferromagnetic ordering in this class of materials. Ferro-ordering occurs when all dipoles are oriented in the same direction, whereas antiferro-ordering involves a ferro-ordering of two or more sublattice in opposite directions.

Ferroelectric materials are commonly used in capacitors, microphones, and transducers due to their large piezoelectric coupling constant [4]. It means that the coupling between an electric field and strain is very strong. Ferromagnetic materials find their application in information processing due to the interaction of electric current and light with magnetic order and also for non-volatile information storage. If we are talking about ferroelectric materials, they exhibit piezoelectric coupling and also they possess memory functionality. The electric polarization remains finite after removing an applied electric field. The information stored in the electric polarization is retained, even after removing the power of the device due to this property. So it can be used in nonvolatile memory devices.

Multiferroic materials can be applied in multiferroic memory devices where the information can be written electrically and read magnetically thus non destructively. Writing the information electrically takes an advantage of lower power operation. To provide this type of memory in microelectronic devices, the materials need to have large coupling between electric and magnetic order, large and switchable polarization and also they need to be highly insulating. It is hard to satisfy these conditions. However, the application of such materials is moving forward. Multiferroic device prototypes are created and being used [5].

To recapitulate, multiferroic materials can be widely used in microelectronics due to their magnetic and electrical properties. However, better characteristics should be achieved for the most applications.

The most widely used multiferroic materials are ABO_3 perovskites. They refer to the type of materials in which ferroic orders arise independently of each other. In this structure class BO_6 octahedra share corners and A-ion is coordinated by eight octahedral (Figure 1).

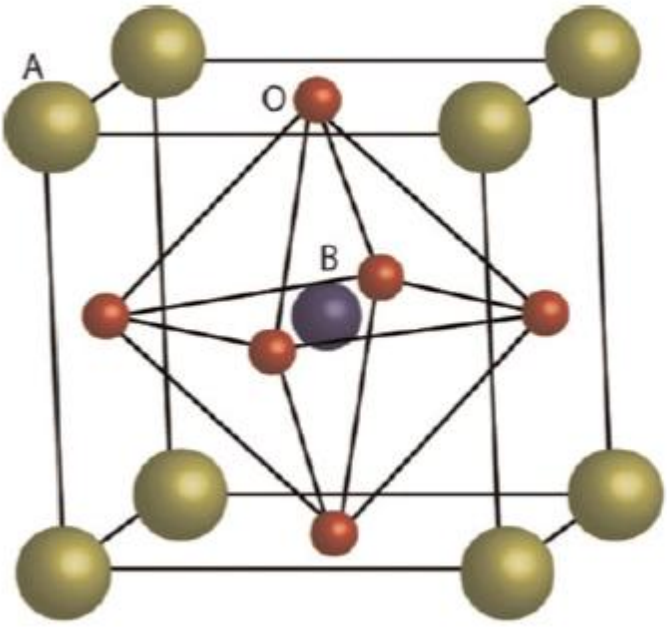

Figure 1. Crystal structure of a perovskite ABO_3 [4].

Typical perovskite ABO_3 is $EuTiO_3$. According to [1] EuTiO3 is Curie−Weiss paramagnetic (PM) at high temperatures. And there is a transition from paramagnetic to antiferromagnetic at the Neel temperature (T_N = 5.5 K). $EuTiO_3$ has perovskite-type crystal structure [6] with Pm-3m space group.

In our research we obtained $EuTiO_3$ from $Eu_2Ti_2O_7$ and investigated their crystal and local structure in order to find the connection between electronic and valence states, crystal structure end local environment. Magnetic properties also depend on local structure of the compound. So the information about their structure makes possible to investigate not this compound but phenomenon in general.

2. Crystal structure of Europium complex oxides

We obtained divalent europium oxides from trivalent europium oxides and investigate them. We had $Eu_2Ti_2O_7$. We annealed it in hydrogen for 4 hours at the temperature of 1000 degrees Celsius. But we decided that it would be interesting to observe a gradual change of the structure. So we annealed our compound again in oxygen at different temperatures to find out how their crystal and local structures depend on their valence. Crystal structure was investigated by X-ray powder diffraction before. We may tentatively conclude that trivalent europium oxides

have a pirochlore-type structure (space group Fd-3m) and divalent oxides have perovskite-type structure (space group Pm-3m). Diffraction patterns can be seen at Figure 2.

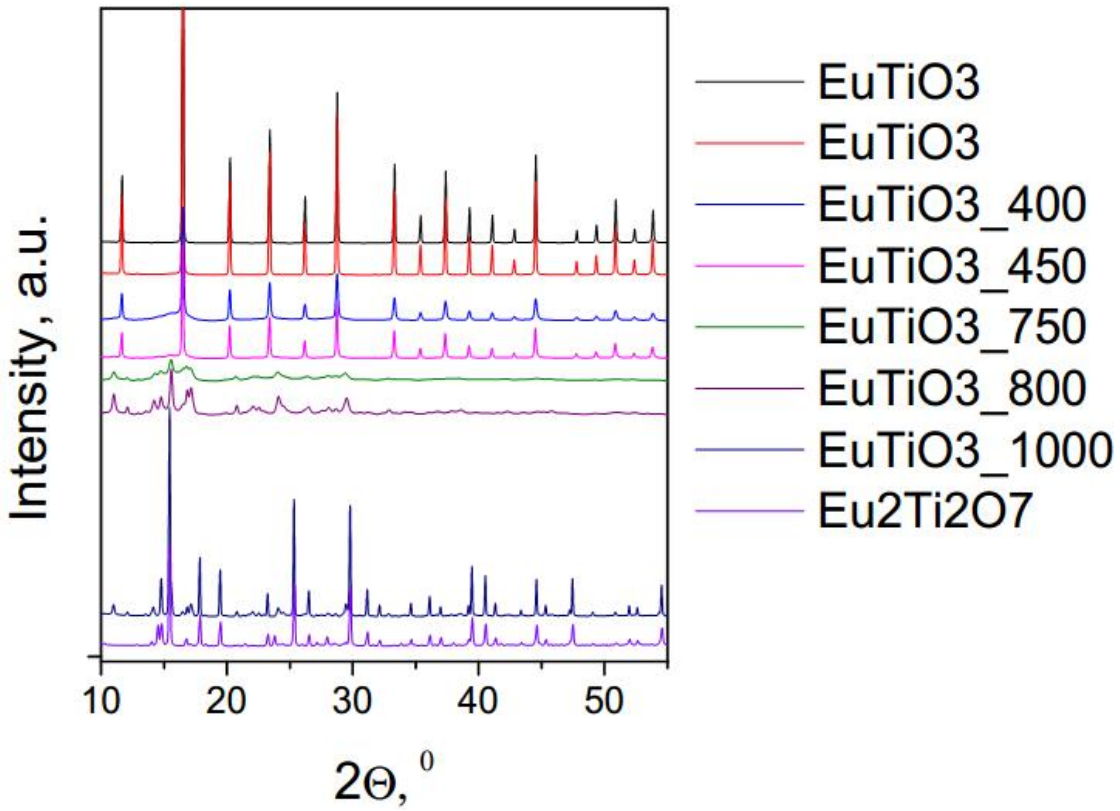

Figure 2. Powder X-ray diffraction data for europium-titanium complex oxides.

Crystal structure does not undergo major changes till ~ 750 ^{0}C. At 750 ^{0}C and 800 ^{0}C we obtained monoclinic crystal structure (space group P21), which was also observed and simulated in [7] and called layered perovskite structure. If we anneal samples at 1000 ^{0}C for 3 hours, we obtain $Eu_2Ti_2O_7$ again with pyrochlore type crystal structure. The same transition of crystal structure is shown at Figure 3.

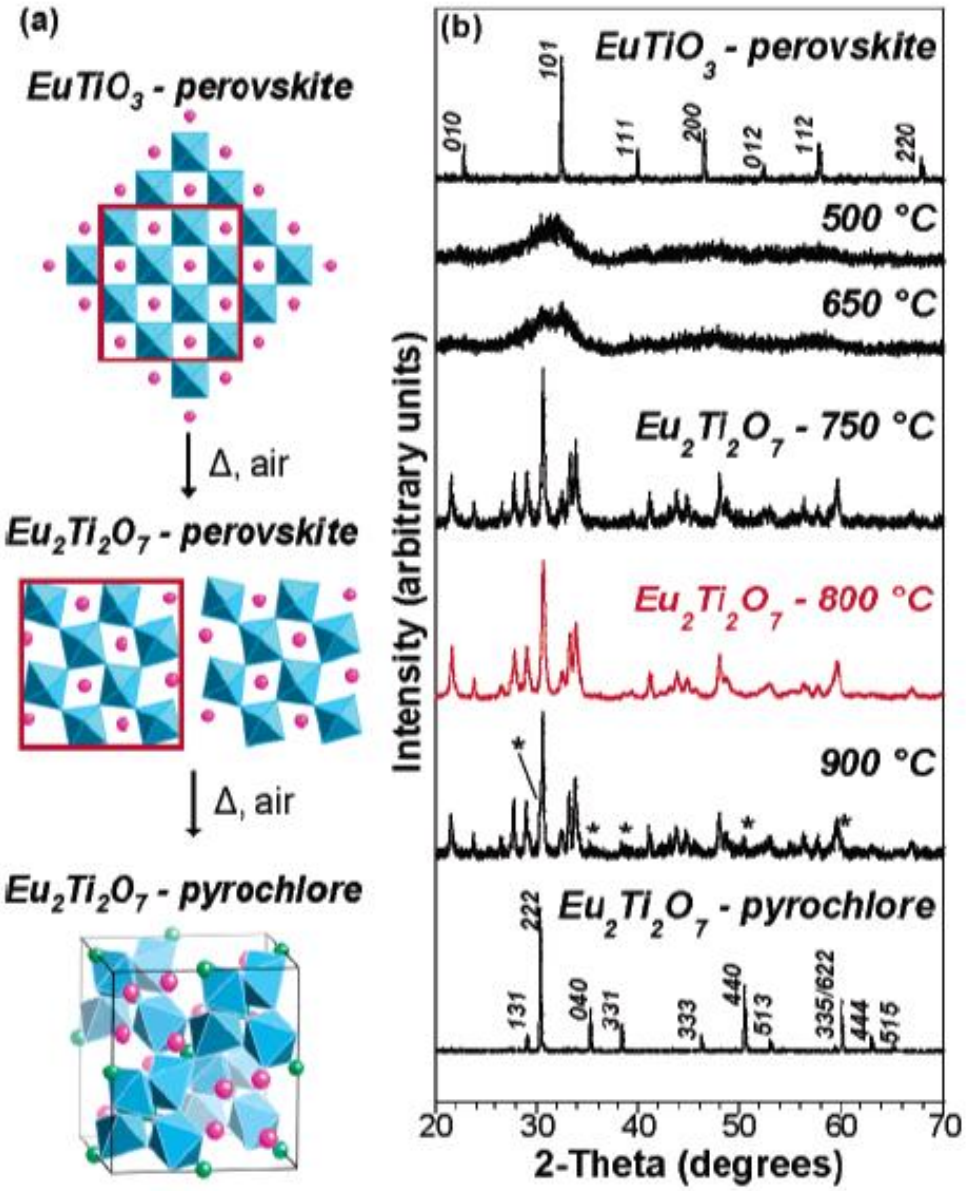

Figure 3. (a) Overview of the transition from $EuTiO_3$ to $Eu_2Ti_2O_7$. The light blue polyhedra represent TiO_6 octahedra, and the pink spheres represent Eu cations. In the pyrochlore structure oxygen atoms that are not part of the TiO_6 octahedra are shown as green spheres.
(b) Powder X-ray diffraction data for the transition from $EuTiO_3$ to $Eu_2Ti_2O_7$ [7].

3. Valence states of Europium complex oxides

Electronic and valence state were investigated using Near Edge X-ray Absorption Spectroscopy (XANES). XANES is a very sensitive method in case of electronic structure investigation due to the dependence of the absorption edge position in energy scale on the valence state.

Valence state of Eu in the compound can be determined by measuring L3 absorption edge of europium (Figure 4(a)). For Eu^{2+} in $EuTiO_3$ the absorption edge position is near 6975 eV, and for Eu^{3+} in $Eu_2Ti_2O_7$ and Eu_2O_3 the absorption edge position is ~ 6980 eV. So we can see an energy shift depended on the valence. For transitional compounds both edges can be seen. The percentage for each valence can be calculated by fitting the spectrum by linear combination of divalent and trivalent europium spectra. The results of such fitting are shown in Table 1.

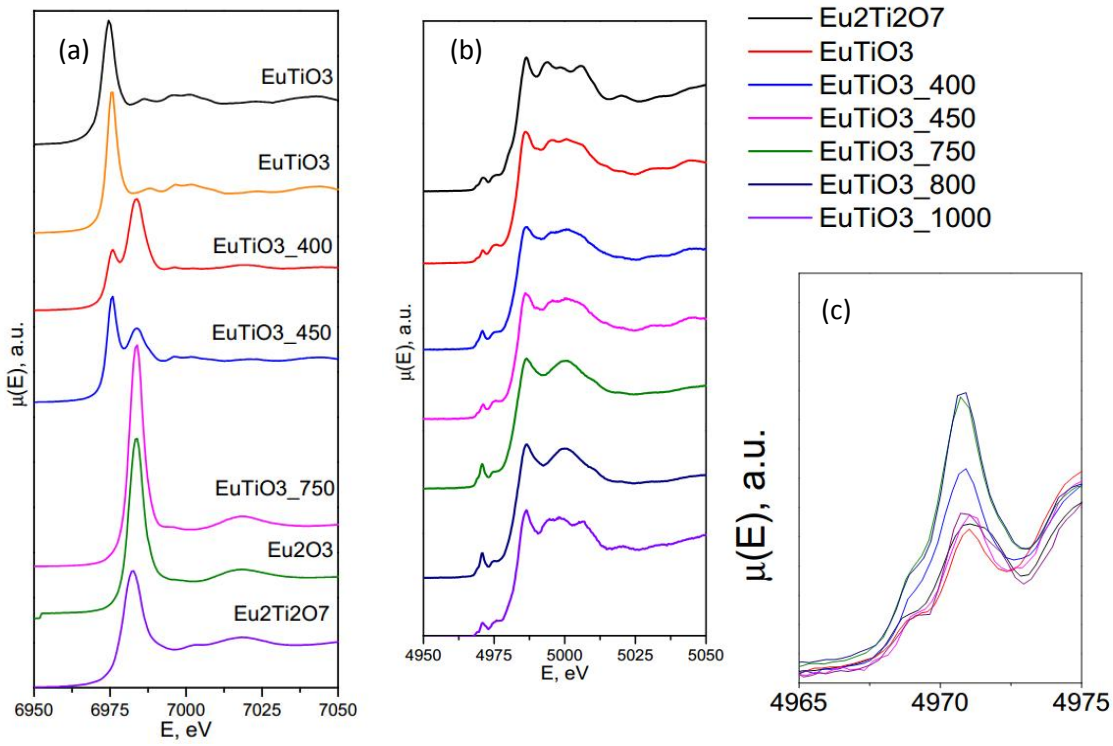

Figure 4. (a) Eu L3-edge XANES spectra of $Eu^{2+}_{(1-x)}Eu^{3+}_{x}TiO_{(3+x/2)}$ compounds after annealing in H_2 and O_2. (b) Ti K-edge XANES spectra of $Eu^{2+}_{(1-x)}Eu^{3+}_{x}TiO_{(3+x/2)}$ compounds after annealing in H_2 and O_2. (c) Pre-edge region of Ti K-edge XANES spectra of $Eu^{2+}_{(1-x)}Eu^{3+}_{x}TiO_{(3+x/2)}$ compounds.

Table 1. Calculation results of the percentage of divalent and trivalent europium in the transitional compounds $Eu^{2+}_{(1-x)}Eu^{3+}_{x}TiO_{(3+x/2)}$.

Compound	**Eu^{2+}(%)**	**Eu^{3+}(%)**	**R-factor (%)**
EuTiO3_400	43,1	56,9	0,5
EuTiO3_450	73,5	26,5	0,08
EuTiO3_750	0	100	2,4

As can be seen from the calculation results and from the Figure 4(a) $EuTiO_3$ annealed at 750 ^{0}C become completely trivalent. However the diffraction data above indicate that crystal structure of this compound cannot become pyrochlore type.

Ti K-edge of the compounds was also measured. As we can see from Figure 4 (b) valence state of titanium in $Eu^{2+}_{(1-x)}Eu^{3+}_{x}TiO_{(3+x/2)}$ does not change during annealing. But from the shape of pre-edge region (Figure 4(c)) we can get the information about crystallization of the sample [8]. High peak in pre-edge region indicates less crystallization of the sample. From figure 4 (c) we can conclude that samples annealed at 750 ^{0}C and 800 ^{0}C are the least crystallized. This result is in a good agreement with the diffraction data discussed before.

For the further discussion it is important to compare XANES spectra of $EuTiO_3$ before and after annealing again (Figure 5). Chemical shift giving us the information about valence state is clearly visible here too. The crystal structure, valence state and crystallization for these compounds are already known. $EuTiO_3$ is well crystallized, it has perovskite-type crystal structure with Pm-3m space group, Eu is divalent in it. $EuTiO_3$ after annealing at 800 ^{0}C is not so crystallized, it has monoclinic crystal structure with P21 space group, Eu is trivalent in it. So in this case, annealing makes the symmetry become lower.

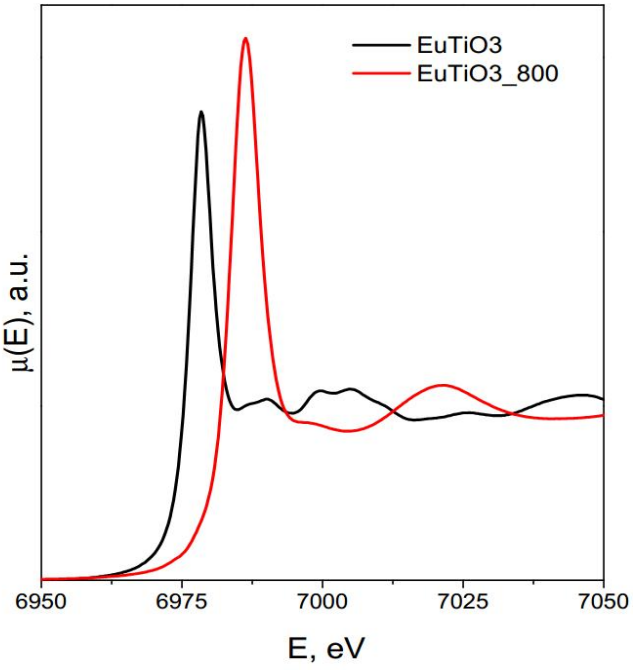

Figure 5. Eu L3-edge XANES spectra of $EuTiO_3$ before and after annealing in oxygen at 800 ^{0}C.

4. Low temperature measurements

4.1. XANES spectra: valence state

From the low temperature measurements the information about interatomic bond stiffness can be extracted [9]. XAFS spectra of $EuTiO_3$ before and after annealing were measured at different temperatures in cryostat. At Figure 6 (a) Eu L3-edge XANES spectra can be seen. There are no major changes in the spectra at different temperatures, as well as in Ti K-edge XANES spectra (Figure 6 (b)). If we look at the pre-edge region of the spectra (Figure 6 (c)), we will not see any temperature caused changes too.

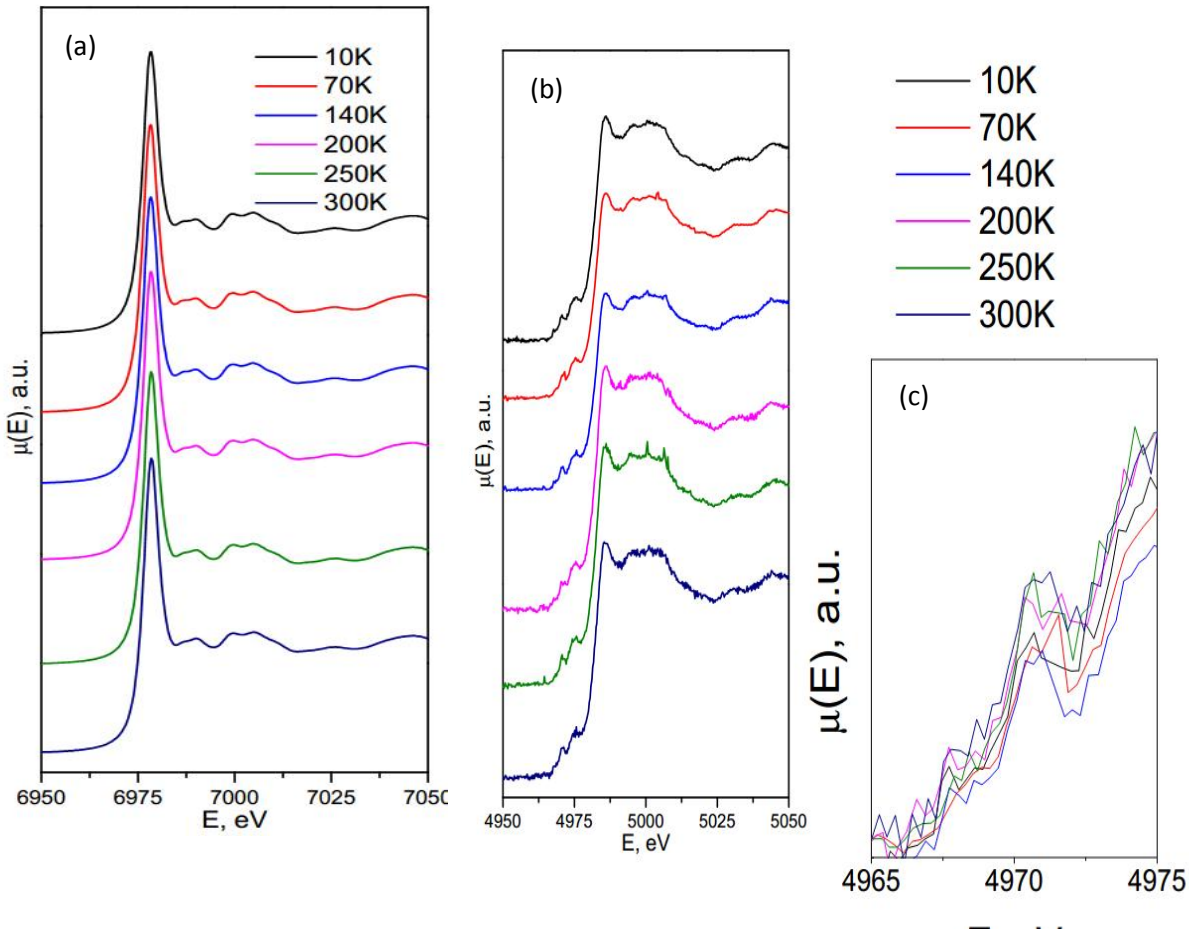

Figure 6. (a) Eu L3-edge XANES spectra of $EuTiO_3$. (b) Ti K-edge XANES spectra of $EuTiO_3$. (c) Pre-edge region of Ti K-edge XANES spectra $EuTiO_3$.

Spectra at Ti K-edge look noisy because it is hard to measure absorption coefficient at such low energies (4966 eV). We need a thin sample with a big amount of absorption element in

it, which is not very easy to produce. But we may tentatively conclude that pre-edge region looks quite similar for each temperature.

The same results we can observe at XANES spectra of $EuTiO_3$ after annealing at 800 ^{0}C. They do not really change with measurement temperature (Figure 7 (a, b, c)).

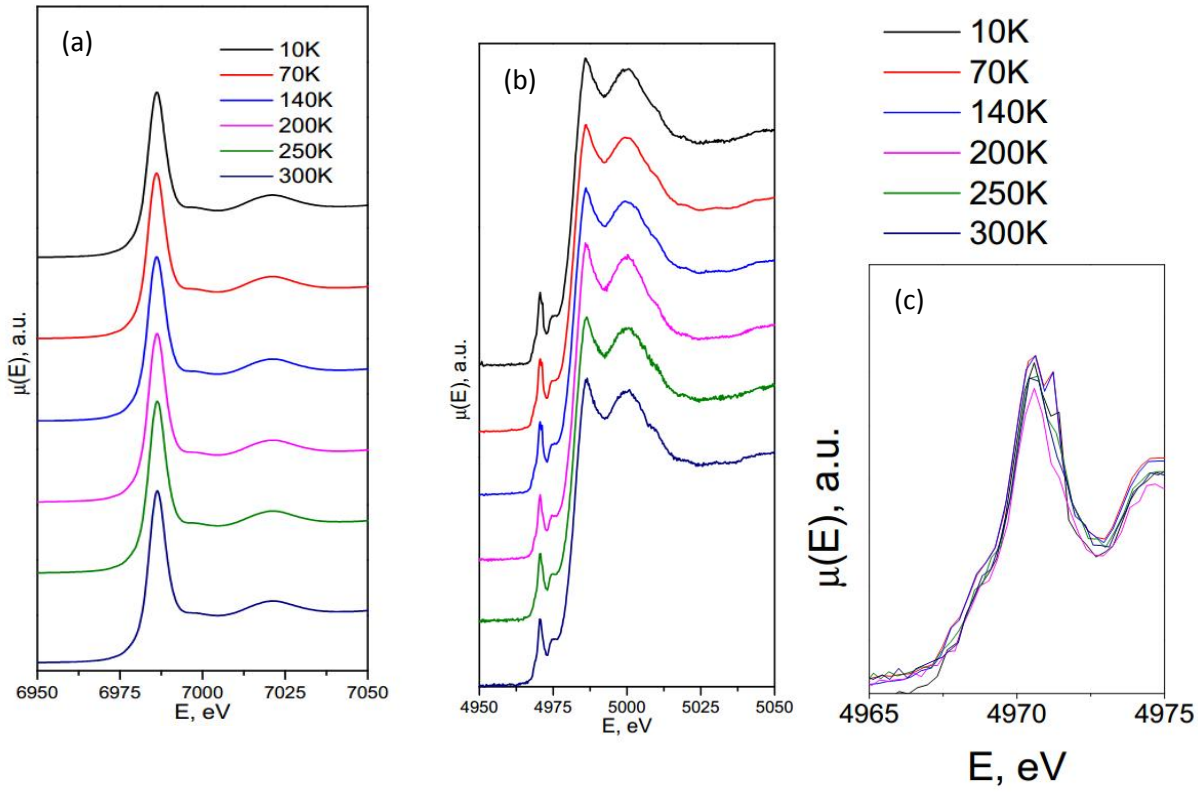

Figure 7. (a) Eu L3-edge XANES spectra of $EuTiO_3$_800. (b) Ti K-edge XANES spectra of $EuTiO_3$_800. (c) Pre-edge region of Ti K-edge XANES spectra $EuTiO_3$_800.

4.2. EXAFS spectra: local structure

The most interesting information here can be extracted from Extended X-ray Absorption Fine Structure (EXAFS). These spectra give us information about local environment of an absorption atom. EXAFS spectra of Eu L3-edge $EuTiO_3$ before and after annealing are shown at Figure 8. From these spectra we can find out the coordination number (N) of the atom, distances to the surrounding atoms (R) and deviations of these distances (σ^2) or Debye-Waller factors which are the characterization of atomic vibrations in the lattice.

To extract information about coordination shells from experimental EXAFS spectrum Fourier transform is being used.

Using model based on EXAFS-function [10] we can calculate parameters discussed above. For such calculations of local environment of the atom we need the information about crystal structure of the compound. Based on the structure data, the amplitudes and scattering phases can be calculated and then used to construct the main EXAFS-function.

For $EuTiO_3$ before annealing there is a high symmetry structure. Each atom of Eu is surrounded by 12 atoms of oxygen in the first coordination shell and 8 atoms of Ti in the second coordination shell according to its structural model. In the calculations coordination number N was fixed, R and σ^2 were fitted. Fitting results are presented in Table 2.

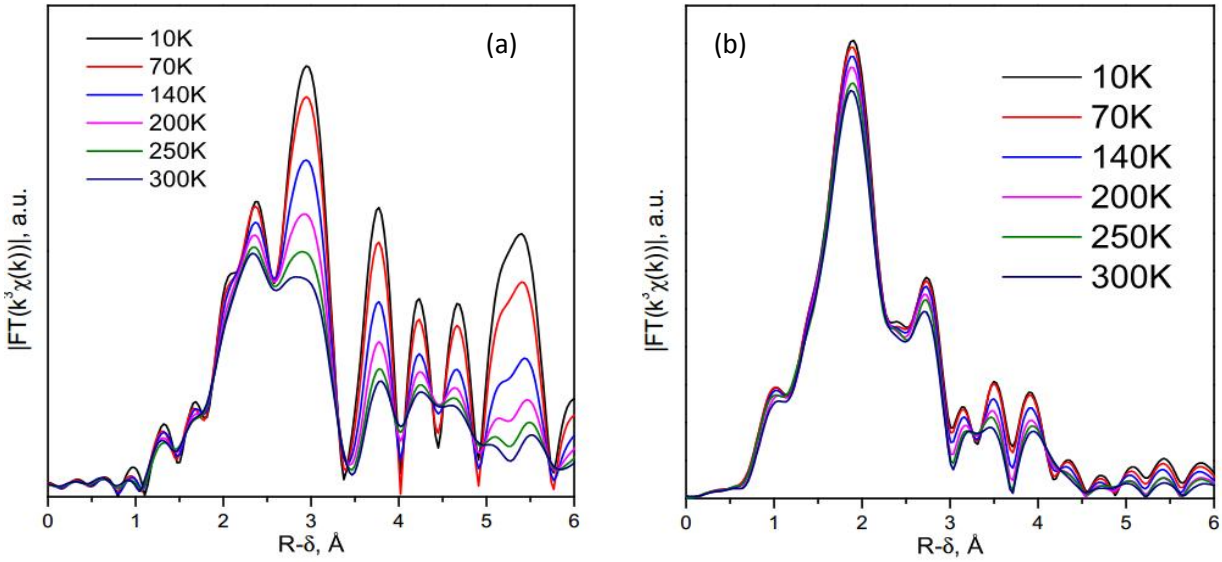

Figure 8. (a) Eu L3-edge EXAFS spectra of $EuTiO_3$ measured at different temperatures. (b) Eu L3-edge EXAFS spectra of $EuTiO_3$ (annealed at 800 ^{0}C) measured at different temperatures.

Table 2. Calculation results of local structure parameters in $EuTiO_3$.

Temperature	Path	N (fixed)	R	sigma2	R-factor
300	Eu-O	12	2.7243	0.0185	0.03855
	Eu-Ti	8	3.3871	0.00757	
250	Eu-O	12	2.7221	0.0182	0.03621
	Eu-Ti	8	3.3836	0.00668	
200	Eu-O	12	2.7178	0.01755	0.03413
	Eu-Ti	8	3.3789	0.00555	
140	Eu-O	12	2.7175	0.01693	0.03106
	Eu-Ti	8	3.3753	0.00422	
70	Eu-O	12	2.7117	0.01637	0.02806
	Eu-Ti	8	3.3703	0.00298	
10	Eu-O	12	2.7118	0.01643	0.02773
	Eu-Ti	8	3.36883	0.00239	

In the Table 2 we can see the gradual change of fitted parameters with temperature. Interatomic distances (Figure 9) and Debye-Waller factors (Figure 10) increase with temperature which caused by thermal expansion and thermal vibrations of atoms.

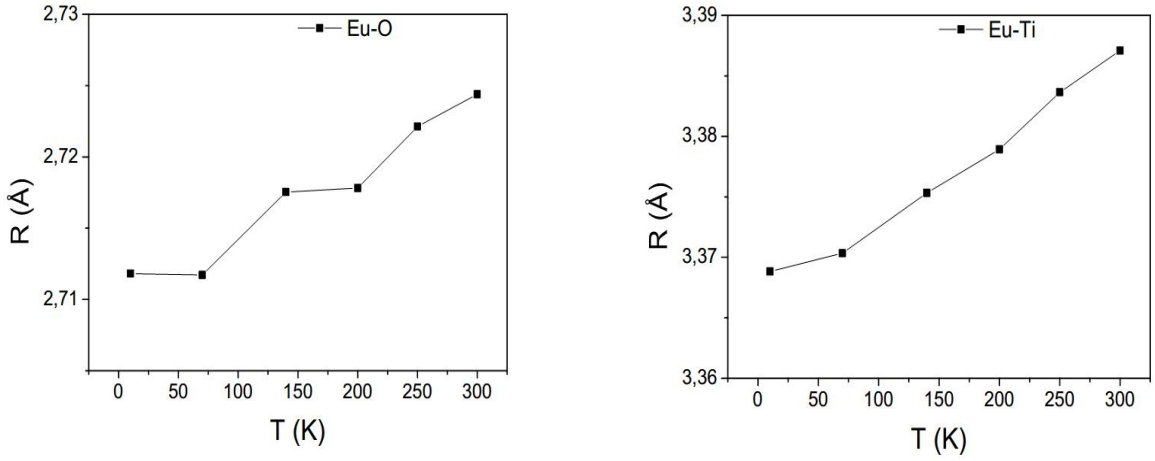

Figure 9. Temperature dependence of interatomic distances for Eu-O bond (left) and for Eu-Ti bond (right).

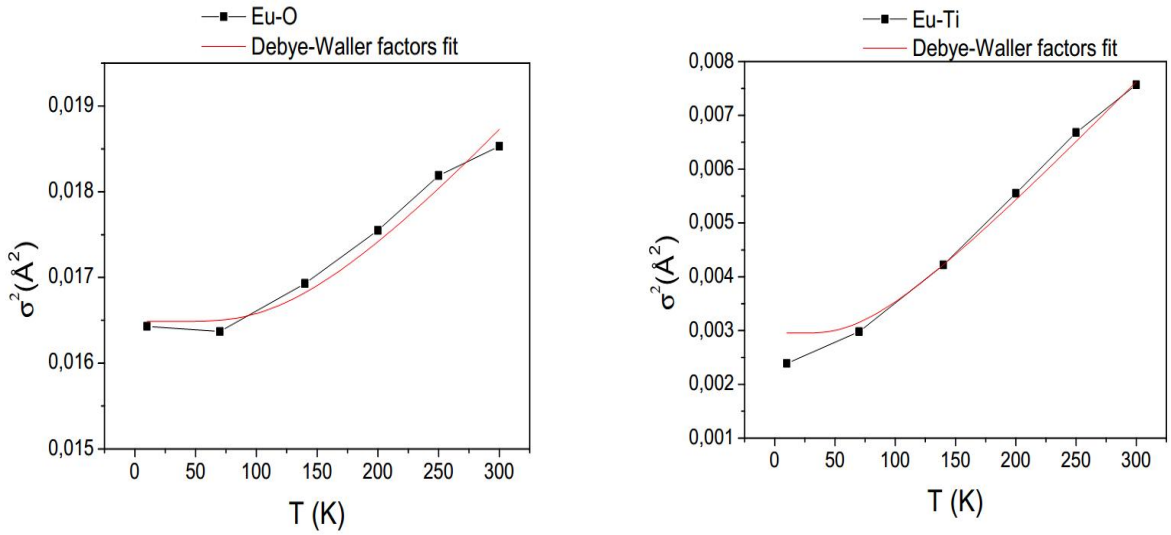

Figure 10. Temperature dependence of Debye-Waller factors for Eu-O bond (left) and for Eu-Ti bond (right).

Temperature dependence of Debye-Waller factors can be described within conventional harmonic model of atomic vibrations:

$$\sigma^2 = \sigma_{stat}^2 + \frac{\hbar^2}{2k\mu}\frac{1}{T_E}coth\left[\frac{T_E}{2T}\right] \quad (1)$$

σ^2_{stat} characterizes the static disorder in the sample crystal structure. σ^2_d characterizes the amplitude of thermal vibrations of atoms. T_E is the Einstein temperature characterizing the interatomic bond stiffness through the effective force constant k_{bond} normalized to the reduced mass μ: $T_E = \sqrt{k_{bond}/\mu}$, ħ is the Plank constant, k is the Boltzmann constant.

Debye-Waller factors are in a good agreement with the Einstein model according to Figure 10. The Einstein temperatures and static Debye-Waller factors determined by simulating the spectra are listed in the Table 3.

Table3. The Einstein temperatures and static Debye-Waller factors for $EuTiO_3$

Interatomic bond	**T_E, K**	**σ^2_{stat}, Å²**
Eu-O	442	0.013
Eu-Ti	236	0.00016

For annealed sample the crystal structure has low symmetry so that the simulation of the EXAFS-function becomes a difficult problem. There are few different positions of Eu in the lattice and it is not possible to distinguish them.

A simplified model was used in this case. We assumed that all interatomic distances are constant and that we can unite different bonds with close distances to one. According to this model there are four O atoms in the first shell at the distance ~ 2.33 Å, then three O atoms at the distance ~ 2.47 Å, then two O atoms and two Ti atoms at the distance ~ 3.28 Å. Oxygen and titanium atoms are also hard to distinguish, so we could look at the temperature changes of only one of them. In the end we fitted Debye-Waller factors of 4 oxygen atoms, 3 oxygen atoms and 2 titanium atoms. Temperature dependence of Debye-Waller factors for the bonds is shown on the Figure 11.

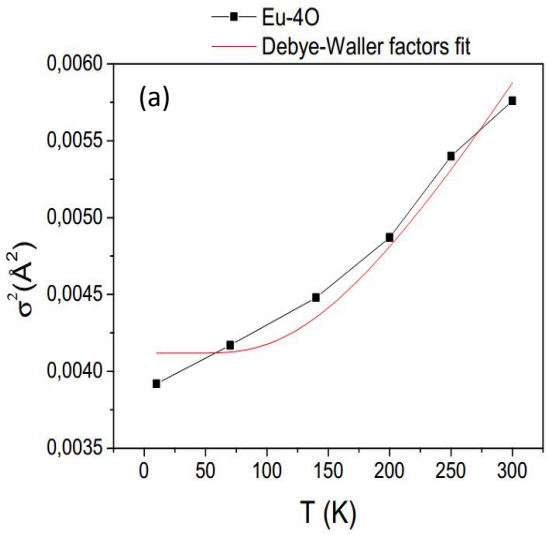

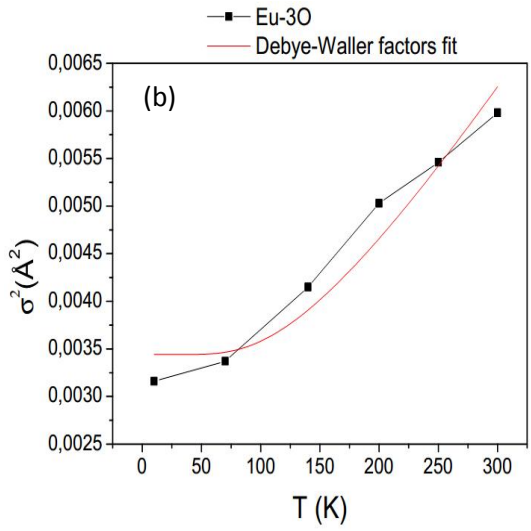

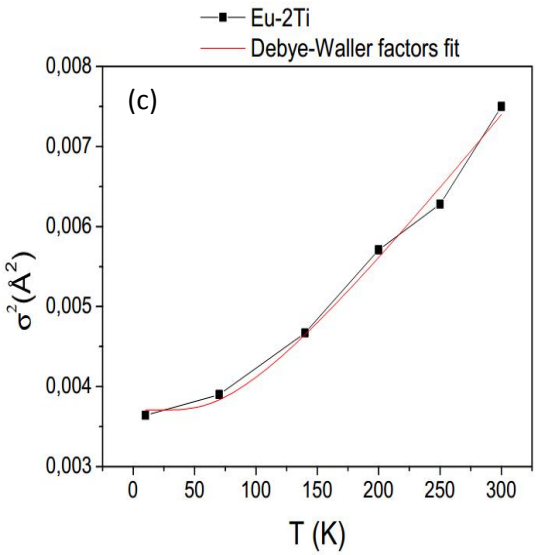

Figure 11. Temperature dependence of Debye-Waller factors for Eu-4O bonds (a), for Eu-3O bonds (b) and for Eu-2Ti bonds (c).

For both Eu-O bonds Debye-Waller factors are not in a good agreement with the Einstein model. However for Eu-Ti bond fit curve is quite close to the experimental one. The Einstein temperatures were calculated for these bonds (Table 4). In this case calculation of the static Debye-Waller factor does not make sense because we add static disorder by choosing absorption element and uniting different bonds to one. So these parameters are not listed in the Table 4.

Table 4. Static Debye-Waller factors for $EuTiO_3$, annealed at 800 ^{0}C.

Interatomic bond	**T_E, K**
Eu-4O	479
Eu-3O	407
Eu-Ti	260

Undoubtedly, these temperatures cannot be considered as Einstein temperatures. Only a qualitative comparison of bond stiffnesses is possible in this case.

5. Conclusion

To recapitulate, we obtained complex oxides with divalent and trivalent Europium and also transitional compounds to consider the gradual change of crystal and local structure of oxides during the valence transition. The connection between valence state and crystal structure was found. We also considered XANES and EXAFS spectra of the compounds at different temperatures to calculate parameters of local structure and interatomic bond stiffnesses, which can be connected to magnetic structure parameters. The purpose of our future work is to finish all required calculations and investigate magnetic properties of the compounds.

6. Acknowledgements

I would like to thank my supervisor, Vadim Murzin, who has helped me in this project, and scientific group P64 for the opportunity to take part in an interesting experiment. Also I would like to thank Summer Program organizing team. DESY summer school has been an amazing experience.

References

[1] H. Akamatsu, K. Fujita, H. Hayashi, T. Kawamoto, Y. Kumagai, Y. Zong, K. Iwata, F. Oba, I. Tanaka, and K. Tanaka, “Crystal and electronic structure and magnetic properties of divalent europium perovskite oxides Eu M O3(M = Ti, Zr, and Hf): Experimental and first-principles approaches,” // *Inorg. Chem.*,2012, vol. 51, no. 8, pp. 4560–4567.

[2] S. Bhansali, C. M. . Sotomayor Torres, and J. Mompart Penina, “Thermoelectric properties of oxides and related materials" // Diss. U. Bern, 2014, 158 p.

[3] A. Bussmann-Holder, K. Roleder, B. Stuhlhofer, G. Logvenov, I. Lazar, A. Soszyski, J. Koperski, A. Simon, and J. Köhler, “Transparent EuTiO 3 films: A possible two-dimensional magneto-optical device,”// *Sci. Rep.*, 2017, vol. 7, pp. 1–6.

[4] A.J.C. Buurma, G.R. Blake, T.T.M. Palstra, “Multiferroic Materials: Physics and Properties”, // Elsevier Inc, 2016, 17 p.

[5] J.F. Scot, “Applications of magnetoelectrics”, // Journal of Material Chemistry, 2012, 22(11), pp. 4567-4574.

[6] J. Kohler, R. Dinnebier, A. Bussmann-Holder, “Structural instability of $EuTiO_3$ from Xray powder difraction”, // Phase transitions, 2012, 10 p.

[7] N.L. Henderson, J.Baek, P.S. Halasyamani, “Ambient-Pressure Synthesis of SHG-Active $Eu_2Ti_2O_7$ with [110] Layered Perovskite Structure: Suppressing Pyrochlore Formation by Oxidation of Perovskite-Type $EuTiO_3$”, // Chemistry of Materials, 2007, V. 19, N. 7, pp. 1883-1885.

[8] V.V. Popov, A.P. Menushenkov, B.R. Gaynanov et.al., “Formation and evolution of crystal and local structure in nanostructures $Ln_2Ti_2O_7$ (Ln = Gd-Dy), // Journal of Alloys and Compounds, 2018, 746, pp. 377-390.

[9] V.V. Popov, A.P. Menushenkov, B.R. Gaynanov et.al., “Local disorder in pyrochlores $Ln_2Ti_2O_7$ (Ln = Gd, Tb, Dy), // Lett. to J.E.T.Ph., 2019, 109, 8, pp. 540-546

[10] Bunker, Grant, “ Introduction to XAFS : a practical guide to X-ray absorption fine structure spectroscopy”, // Cambridge: Cambridge University Pres, 2010